Quantitative Assessment of Compressed-Sensing Reconstruction Fidelity for 3D He-3 and H-1 Acquisitions in One Breath-hold

Kun Qing[1], Talissa A. Altes[2], Nicholas J. Tustison[2], Jaime F. Mata[2], G. Wilson Miller[2], Eduard E. de Lange[2], William A. Tobias[3], Gordon D. Cates[3], James R. Brookeman[2], and John P. Mugler[2]

[1]*Biomedical Engineering, University of Virginia, Charlottesville, VA, United States,* [2]*Radiology and Medical Imaging, University of Virginia, Charlottesville, VA, United States,* [3]*Physics, University of Virginia, Charlottesville, VA, United States*

Introduction: Rapid acquisition of 3D He-3 and H-1 image sets within one breath hold has been implemented by randomly undersampling the 3D *k* space, and applying compressed-sensing (CS) reconstruction [1,2]. Although consistency between the fully-sampled and CS image sets was verified by visual comparison, as well as indirectly by using undersampling and reconstruction of fully-sampled image sets [3], direct quantitative comparison of the two image sets is difficult because they are typically obtained in different breath holds. In this work, we sought to directly and quantitatively evaluate the reconstruction fidelity of the undersampled CS 3D image sets by acquiring both the fully-sampled and undersampled acquisitions for a given nucleus (He-3 or H-1) in the same breath hold.

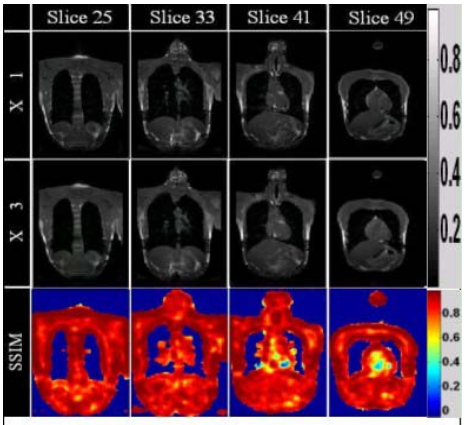

Fig.1. Comparison of representative images from fully-sampled (top row) and undersampled at R=3 (second row) H-1 acquisitions obtained in one breath hold.

Methods: *Experimental setup*: Helium and proton studies were performed using a 1.5-T whole-body scanner (Avanto, Siemens Medical Solutions) equipped with the multi-nuclear option and a chest He-3 RF coil (Rapid Biomedical). He-3 gas was polarized by collisional spin exchange with an optically-pumped rubidium vapor using a prototype commercial system (Magnetic Imaging Technologies, Inc.). All experiments were performed under a Physician's IND (#57866) for imaging with hyperpolarized He-3 using a protocol approved by our institutional review board. Informed consent was obtained in all cases. *Pulse sequences*: A 3D balanced steady-state free-precession (TrueFISP) sequence was used for both He-3 and H-1. Parameter settings included: He-3: TR/TE 1.86/0.79 ms, matrix 128x88x52; and H-1: TR/TE 1.79/0.74 ms, matrix 128x110x64. Common parameters for both scans were: flip angle 9°, spatial resolution 3.9x3.9x3.9 mm, bandwidth/pixel 1085 Hz. Total acquisition time was 2.8 s for He-3 and 4.1 s for H-1 at three-fold acceleration (R=3), compared with 6.7 s for He-3 and 9.7 s for H-1 for the fully-sampled scans. *Compressed-sensing setup*: Undersampling patterns were generated using a MonteCarlo algorithm, as described by Lustig et al [2]. The Cohen-Daubechies-Feauveau 9/7 (CDF 9/7) wavelet was used as the sparsifying transform. All CS reconstructions were implemented in MATLAB (The Mathworks, Natick, MA). Performance of the CS reconstruction was evaluated using mean absolute percentage error (MAPE) and the structural similarity (SSIM) index. *Human studies*: One healthy subject was scanned using the H-1 protocol with full sampling and undersampling (R=3) in a single breath hold; the undersampled data was acquired first. Similarly, three healthy subjects were scanned using the He-3 protocol with full sampling and undersampling (R=3) in a single breath hold. For the first two subjects, the undersampled data was acquired first, the same as for H-1, while for the third subject, an additional fully-sampled data set was acquired (acquisition order: fully sampled, undersampled [R=3], fully sampled; flip angle 7.9° for optimal SNR).

Results & Discussion: Results from the H-1 comparison are presented in **Fig. 1**, with the upper row showing representative images for full sampling and the middle row showing corresponding images reconstructed from undersampled data. In general, a high level of similarity was found between the two image sets, as indicated by a MAPE of 9.6% and mean SSIM index of 0.90 over all signal-containing regions in the 3D coronal slices. These values are very similar to those calculated by applying the same undersampling pattern to fully-sampled data and then comparing the resulting CS-reconstructed images to the original fully-sampled images. In contrast, the similarity values for the He-3 acquisitions were not as good as those for the H-1 acquisitions: the MAPE and SSIM values calculated by comparing the fully-sampled (first for the third subject) and undersampled image sets were 17% and 0.72, and 16% and 0.74, respectively, for the first two subjects (FA 9°), and 13% and 0.77, respectively, for the third subject (FA 7.9°). The relatively lower indices obtained for He-3 appear to arise from at least 2 factors unrelated to the actual performance of the undersampled acquisition with CS reconstruction: (1) diaphragm movement between acquisitions, which can be clearly seen in the difference images in the 3rd row of **Fig. 2** (scaled to the maximum of each image), where a relatively large signal difference is present at the lung-diaphragm interface; and (2) the non-equilibrium nature of hyperpolarized-gas magnetization and B1 inhomogeneity of the RF coil. Since undersampled and fully-sampled datasets are acquired sequentially, the signal intensity decreases roughly 15-20% for the second He-3 acquisition, based on the flip angle used, while noise remains constant from acquisition to acquisition. Also, B1 inhomogeneity gradually modifies the relative signal-intensity distribution within ventilated regions of the lung. These factors may explain the relatively low SSIM indices appearing in most of the uniformly-ventilated regions of the lung (4th row of **Fig. 2**), while in regions containing vessels or edges, the similarity indices are much higher. CS-reconstruction of data from the fully-sampled image set offers further insight on these issues: after applying the undersampling pattern with R=3, the CS-reconstructed image yields a MAPE of 8.1% compared with the fully-sampled image, while the SSIM index is 0.882. After adjusting the signal intensity at each pixel of the reconstructed undersampled image based on a B1 map acquired simultaneously with the image data, the MAPE increases somewhat to 8.8%, while the SSIM index decreases to 0.879. Then, adding noise at a level consistent with the consumption of magnetization during the actual acquisition, the MAPE increases to 12.9%, while the SSIM index decreases to 0.810; these values are close to the best indices from the real comparison. This suggests that both B1 inhomogeneity and SNR loss (due to consumption of the hyperpolarized magnetization) affect the comparison, with SNR being the larger factor. The effects of these factors is also supported by comparison of the two fully-sampled data sets acquired in subject 3, which yields a MAPE of 23% and a SSIM value of 0.68; both of these values are worse than those for the fully-sampled vs. undersampled He-3 data.

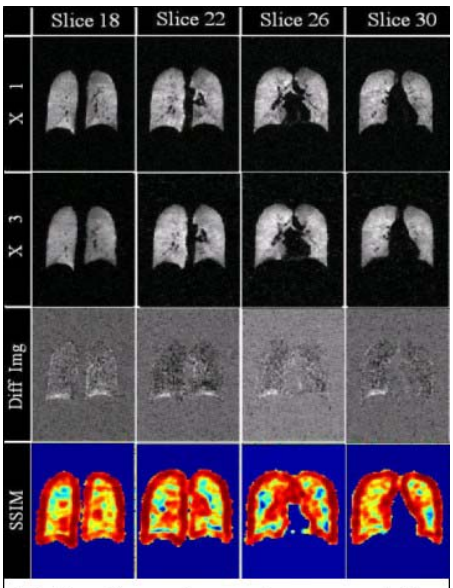

Fig.2. Comparison of representative images from fully-sampled (top row) and undersampled at R=3 (second row) He-3 acquisitions obtained in one breath hold.

Conclusions: Undersampled, CS-reconstructed H-1 3D images showed high similarity to their fully-sampled counterparts. While somewhat lower similarity indices were found for undersampled, CS-reconstructed He-3 3D image sets, we believe this arises from factors unrelated to the actual performance of the undersampled acquisition with CS reconstruction, including diaphragm movement during the acquisition, the non-equilibrium nature of hyperpolarized magnetization, and B1 inhomogeneity.

References: [1] Qing K et al. Proc ISMRM 19 (2011): 546. [2] Lustig M et al. Magn Reson Med 2007;58:1182. [3] Ajraoui S et al. Magn Reson Med 2010;63:1059.

Acknowledgements: This work was supported by NIH R01 HL079077 and Siemens Medical Solutions.